

RESEARCH ARTICLE

Open Access

# Real-world application of a discrete feedback control system for flexible biogas production



Lingga Aksara Putra<sup>1\*</sup> , Bernhard Huber<sup>1</sup>  and Matthias Gaderer<sup>1</sup> 

\*Correspondence:  
lingga\_aksara.putra@tum.de

<sup>1</sup> Technical University of Munich,  
Professorship of Regenerative  
Energy Systems, Schulgasse 16,  
94315 Straubing, Germany

## Abstract

Using renewable energy is increasingly prevalent as part of a global effort to safeguard the environment, with a reduction in CO<sub>2</sub> being one of the primary objectives. A biogas plant provides an opportunity to produce green energy, but its profitability prevents it from being utilized more frequently. A suitable response to this economic issue would be flexible biogas production to exploit fluctuating energy prices. Nevertheless, the complex nature of the anaerobic digestion process that proceeds within the biogas plant and the wide range of substrates that may be utilized as the plant's feeds make it challenging to achieve flexible biogas production truly. Most plant operators will rely on their experience and intuition to run the plant without knowing exactly how much biogas they will produce with the feed substrate. This work combines a system model estimation and feedback controller to provide an intuitive yet precise feedback control system. The system model estimation represents the biogas plant mathematically, and a total of six distinct approaches have been compared and evaluated. A PT1 model most accurately approximated the step-down and the step-up by the time percentage method, with the Akaike Information Criterion as the primary evaluation criterion for selecting the best model. The downward model was controlled by a discrete PI controller modified with the Root Locus Method and an Anti-Windup scheme, and the upward model was controlled by a state space controller. The quality of the controller was evaluated in both simulation and at the actual biogas plant in Grub, and the controller was able to reduce the biogas production rate approaching the setpoint in the expected period. Furthermore, the developed feedback control system is effortless enough to be installed in many biogas plants.

**Keywords:** Model estimation, Discrete controller, Feedback control system, Flexible biogas production, Anaerobic digestion

## Introduction

Alternatives to fossil fuels are essential for the continued sustainability of our planet. The country amended the (Renewable Energy Sources Act) with the EEG to provide the groundwork for Germany to achieve carbon neutrality more quickly. One of the key objectives is to reach at least 80% renewable energy coverage of gross power consumption by 2030 [1, 2]. To replace fossil fuels with more ecologically friendly and sustainable forms of energy generation, biogas plants must be considered an alternative.

A biogas plant is a facility where anaerobic digestion may take place. Five primary sections comprise a biogas plant: Substrate management area, Feeding area, Anaerobic digestion area, Gas storage area, and Digestate storage area [3, 4]. The substrate management area stores biogas substrates consisting of animal dung, residual garbage, and renewable resources like maize and grass silage.

The heart of the plant, where fermentation occurs, is the anaerobic digestion section. Fermentation includes the hydrolysis phase, the acidogenic phase, the acetogenic phase, and the methanogenic phase [5]. These are referred to as the "four phases of degradation," and methane is produced as a result. The gas storage facility will hold the produced methane or biogas until needed. Usually, the gas will be sent to a combined heat and power (CHP) facility, where it will be converted into electricity and heat.

Electricity and gas prices fluctuate more due to Russia's invasion of Ukraine, and running a biogas plant without government support in Europe is becoming increasingly unprofitable. Thus, it is necessary to find strategies to find new feasible business models for biogas plants. The ability to maximize the production of sustainable energy while also providing financial benefits to the owners of biogas plants is one of the significant advantages of having flexible biogas production. The initial step in achieving this flexibility is creating a mathematical biogas plant model and a suitable feedback control system.

### Literature overview

First, a system model of the biogas plant must be created. The White-Box, Grey-Box, and Black-Box methods can be used to construct a system model. The White-Box approach necessitates an understanding of physiology and fundamental system analysis. The ADM1 model [6], based on an anaerobic digester's biochemical and physiochemical processes, is the most widely used biogas plant model from the White-Box method.

Due to its widespread adoption, the ADM1 model has undergone various modifications. For instance, it has been extended to simulate thermophilic anaerobic digestion of thermally pretreated waste-activated sludge [7], to simulate methane production and volatile fatty acid (VFA) concentrations at different ammonium concentrations [8], for the discontinuous feeding process [9], and for modeling municipal primary sludge hydrolysis [10].

The precision of this model is what gives it its popularity, but its tremendous complexity comes at a cost. If exclusively differential equations express the model, the ADM1 model has 32 dynamic concentration state variables. As a result, various studies have been done to simplify the ADM1 model [11–14]. Additionally, different investigations were conducted to calibrate the ADM1 model in a steady state to minimize the model complexity [15, 16].

Another significant drawback from a practical standpoint is the necessity of measuring several states and characteristics, mostly with laboratory equipment. This issue has been addressed in a variety of methods, including by using Biochemical Methane Potential (BMP) test data for calibrating the model [17] and using a biochemical or kinetic parameter estimation approach in batch experiments [18–21].

On the other hand, there have been experiments to estimate parameters using mathematical estimation methods, including particle swarm optimization [22], the aspen plus constrained simplex derivative-free algorithm [23], the combined

correlation-based parameter estimation with sequential single parameter estimation [24], Kalman Filter [25, 26], Robust Internal Observer [27], and Sliding Mode Observer [28].

Despite all the advancements, finding an adequate White-Box method model is still challenging because it either has an excessive level of complexity or many restrictions on its use. Even if a completely functioning model using the White-Box method can be developed, it still does not consider the digester's mixing quality, which might significantly impact biogas output [29–31].

This indicates that to develop a 3D model of the anaerobic digestion process in the digester, the White-Box model must be expanded to include space–time dynamics using a system of partial differential equations [32, 33]. Developing a feedback control system for such a complicated system with space–time dynamics is challenging. This model is frequently constructed to establish a digital twin of the biogas plant rather than to design a system model for a feedback control system.

The high complexity of the system model is one of the main justifications for modeling a biogas plant using the Black-Box method. Using statistical data, this approach looks for a connection between input and output, in this example, between substrate feeding and biogas generation. The most frequently utilized technique for predicting biogas production using this method is incorporating artificial intelligence (AI) [34–37]. The most significant drawback, nevertheless, is the volume of data required. The data collection required for this Black-Box method to develop a model will take ample time.

As a result, this paper proposes employing the Grey-Box method to represent the biogas plant system. Combining both strategies, the Grey-Box method may benefit from the best of both worlds. The primary concept behind this strategy is to estimate the parameters using the data (Black-Box method) and the model structure from the White-Box method. This concept has been tried [38–40], but the algorithms were solely tested on a test plant or simulation, not an actual biogas plant. Additionally, the concept has only been studied for a single substrate. It is still unknown how different substrate interactions would affect the results.

The feedback control may be constructed once the system model has been established. It is the typical procedure to either utilize the traditional way from control theories, such as PI-Controller [41] and PID-Controller [42], or to employ modern approaches, such as Model Predictive Control (MPC) [43–45]. At first glance, utilizing MPC rather than a traditional PI(D)-Controller should yield superior control outcomes since MPC is a multivariable discrete controller that can manage restrictions. However, according to Haugen et al. [46], the performance of MPC is only significantly superior to PI-Controller in setpoint tracking. If the setpoint is constant, the PI-Controller competes well with the MPC. Given that the setpoint can typically be considered consistent for a given amount of time and that installing a PI-Controller in an actual biogas plant is significantly easier than an MPC, it's unquestionably a substantial advantage for the classical controller.

The real-world implementation of a feedback controller is crucial in determining which feedback control system needs to be further investigated. Therefore, experimenting with a fuzzy logic control system makes perfect sense [47, 48]. Implementing a Fuzzy Logic Control System is undeniably a viable option. Yet, the controller may be unstable since the Fuzzy Control relies on human experience, often that of the plant operator. If

the plant is in a situation where something has yet to occur before, fuzzy control may result in a non-optimal control, and the control outcome may be nonsensical.

## Methods

The project's primary objective is to develop a feedback control system for demand-driven biogas production. The control system must be precise enough to operate the biogas plant and simple enough to be installed in many biogas plants and used by the plant manager. This section comprises biogas plant and feeding substrates, data preprocessing, model estimation, and feedback control design.

### Methods 1: Biogas plant and feeding substrates

The system model and the feedback control system will be compared and evaluated in the biogas plant Grub. The Free State of Bavaria commissioned the construction of the biogas plant Grub, one of Germany's most cutting-edge agricultural biogas plants. The plant consists of a 75 kW gas engine CHP unit, a 1206 m<sup>3</sup> digester with concrete cover, and 2714 m<sup>3</sup> fermentation residue storage [49].

Siemens Programmable Logic Controllers (PLC) control the plant semi-automatically. This implies that although the plant has an automated feeder, the plant operator must manually determine how many substrates will be supplied. The PLC also provides access to sensors installed in the plant for temperature, pressure, and gas flow rate.

The feeding substrates used by this plant include slurry (liquid manure), corn, cattle manure, sheep manure, grass silage, and fodder residues. The biogas plant Grub is often supplied with many substrates at once, unlike many lab-scale biogas plants employed in the literature. The primary issue with many studies is that the models are only created for inputs of a single substrate rather than for combinations of many substrates (substrate mixtures).

Instead of utilizing each substrate individually as input, this study suggests using the substrate mixtures as one input of the system model with the Grey-Box method. For instance, the substrate combinations in the biogas plant Grub include slurry, corn, manure, grass silage, and fodder residues (Table 1). The slurry is continuously fed to the plant, and the remainder can be blended as follows:

The percentages are selected with the plant operator's advice rather than randomly. The plant operator can define multiple substrate combinations that may be supplied to the plant. Different substrate combinations are required since the feeding constantly depends on the feeding storage. For example, in the event of adverse weather, substrate mixture 1 ( $u_1$ ) will be utilized if access to substrate mixture 2 ( $u_2$ ) with 70% corn is not possible.

**Table 1** Substrate mixtures in the biogas plant Grub

Substrate mixtures, $u$	Corn	Manure	Grass silage and fodder residues
1	55%	33%	12%
2	70%	25%	5%
...	...	...	...

## Methods 2: data preprocessing

Before designing the feedback control system, the biogas plant's system model must first be created. As previously noted, this paper suggests using the Grey-Box method to estimate the plant.

The Grey-Box method combines the White-Box method, which employs an analytical and physical description of the plant, and the Black-Box method, which relies purely on statistical correlation. The White-Box method necessitates the usage of the ADM1 model, which, when implemented as a system of differential equations, has 32 dynamic concentration state variables. Several laboratory measurements are then required to measure all the necessary parameters to complete the ADM1 model. The Black-Box model analyzes statistical data to assess the relationship between input and output data. This paper uses first and second-order differential equations as the basic model. The concept originated from the ADM1 model, which mainly comprises first and second-order differential equations. Then, the model's parameters are determined based on the relationship between input and output data. The modeling method used in this paper is a Grey-Box method since the structure of the model derives from the White-Box method, and the model parameters are estimated using the Black-Box method without performing any laboratory measurements.

The model's (Fig. 1) input is the rate at which the substrate mixture is fed ( $u$ ) and its output is the rate at which biogas is produced ( $y$ ). In actuality, the production of biogas depends not only on the feeding of the substrate but also on the condition of the plant, such as temperature, the amount of dry matter present, and the ratio of volatile fatty acids to total alkalinity (VFA/TA ratio).

However, the PLC's temperature control ensures that the digester's temperature stays consistent. The dry matter content is approximately 10%, and the VFA/TA ratio is around 0.2. This was the outcome of samples obtained over time from the biogas digester and measured in a lab. As a result, it is possible to consider the biogas plant's status to remain constant for the time being or to alter minimally. These constraints, which will be described in greater detail later, can be considered the system model's operating point.

The step method from control theory is suggested in this study as a way to construct a mathematical connection between input ( $u$ ) and output ( $y$ ). A step denotes a significant change, and when an input is abruptly changed, the output will show a step response. Based on this step response, a differential Eq. (1) can be derived that represents the output trajectory.

$$a_n \frac{d^n y}{dt^n} + a_{n-1} \frac{d^{n-1} y}{dt^{n-1}} + \dots + a_1 \frac{dy}{dt} + a_0 y = b_0 u + b_1 \frac{du}{dt} + \dots + b_{m-1} \frac{d^{m-1} u}{dt^{m-1}} + b_m \frac{d^m u}{dt^m}. \quad (1)$$

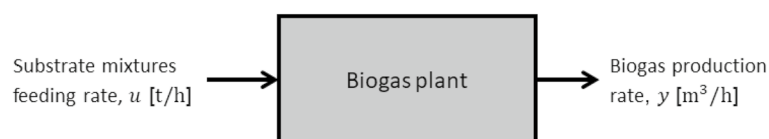


**Fig. 1** System model based on the Grey-Box method

It is vital to remember that biogas creation is a latent and slow process before adopting the step method in the biogas plant. Not only does the present input affect the gas production, but also the historical input from the previous hours or days. As a result, advanced planning is required.

For instance, the biogas plant was fed with the substrate mixture 1 (Table 1) during the experiment with the following scenario:

- $9 \frac{t}{d}$  for Sunday–Wednesday: consisting of  $5 \frac{t}{d}$  corn,  $3 \frac{t}{d}$  manure, and  $1 \frac{t}{d}$  Grass silage and fodder residues.
- $3 \frac{t}{d}$  for Thursday–Saturday: consisting of  $1.66 \frac{t}{d}$  corn,  $1 \frac{t}{d}$  manure, and  $0.33 \frac{t}{d}$  Grass silage and fodder residues.

This scenario ensures that there was no significant change in the substrate feeding rate prior to the desired step. Subsequently, this scenario was applied at the biogas plant Grub, and the results of a downward step action (beginning at approximately 08:00 on Thursday, 29 September 2022) were as follows (Fig. 2).

The blue line on the graph's left ordinate shows the biogas production rate, while the red line on the right ordinate represents daily accumulated substrate mixture feeding. The abscissa contains date and time information, and the experiment was carried out between 29 September and 1 October 2022. Nonetheless, it is difficult to determine the step and the step response. Preprocessing procedures must thus be conducted.

First, preprocessing will be performed on the measured biogas production rate. On this measurement, a high amplitude of noise is visible. This leads to discrete low-pass and smoothing filters [50, 51]. Low-pass filters allow signal components below their cut-off frequency to pass almost unattenuated while attenuating higher-frequency components. The low-pass filter's primary function is to reduce the most prominent peaks every  $2/3$  h. The mixing processes cause these systematic and periodic peaks. This low-pass cut-off frequency has been determined so that the peak frequency will be 60 dB weakened. Subsequently, the data will be flattened using the moving average filter.

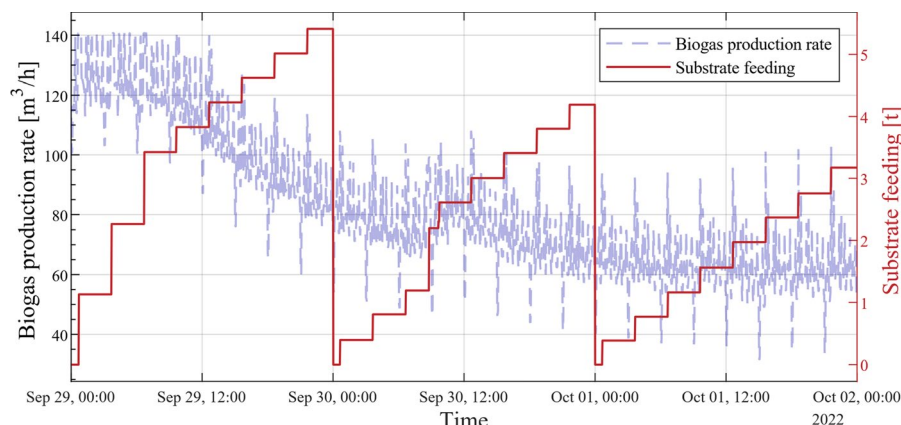


**Fig. 2** Biogas production rate and substrate feeding before preprocessing

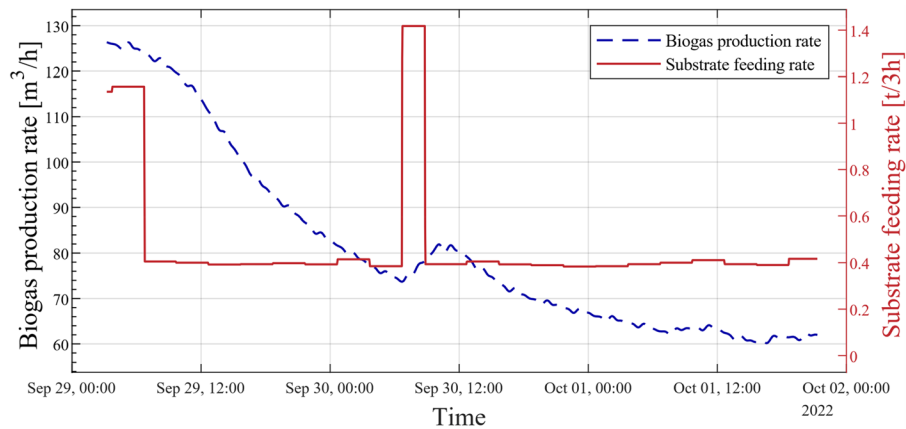


**Fig. 3** Biogas production rate and substrate feeding rate after preprocessing

Substrate mixture feeding will then undergo preprocessing. It can be recognizable in Fig. 2 that the value of this daily accumulated substrate feeding is reset at midnight. Therefore, the substrate feeding's absolute value does not provide much information. The feeding rate is the critical information that must be extracted from this measurement. The first-order discrete derivative will thus be carried out. In this case, only positive derivatives are considered. Since negative derivatives are just the outcome of the reset action at midnight. Due to non-causality and the potential to amplify noise, using a derivation on actual data is only occasionally advised. Therefore, following the derivation, further processing steps must be conducted to ensure the output is coherent and consistent.

To complete the preprocessing step, both data sets will be resampled and interpolated into one time series (Fig. 3).

The discrete derivative of the measured substrate feeding provided the substrate feeding rate (red line). Here, the experiment's step is identifiable. On 29 September, the substrate feeding rate substantially decreased from around  $1.19 \frac{t}{3h}$  to roughly  $0.4 \frac{t}{3h}$ . The plant operator was in charge of the unanticipated increase on 30 September since it was a Friday, and preparations for the weekend were underway. This will be deemed a disruption and will be covered in greater depth in the next section.

The biogas production rate (blue line) is the response to the abrupt change in the substrate feeding rate. The filtered data still contains a negligible amount of noise. Nonetheless, the amplitude is low and only affects the measurement inadequately.

### Methods 3: model estimation

The system model will now be estimated using the filtered measurement data. Several estimating techniques, including the PT1-approximation, time percentage method, turning tangent method, the sum of time constants method, PT1-estimator, and PT2-estimator [52–54], have been examined in this research. For clarity, only the PT1-approximation and the time percentage method are discussed in detail in this subsection.

**PT1-approximation**

PT1-approximation refers to using a first-order differential equation to predict the trajectory of the biogas production rate Eq. (2).

$$T \cdot \frac{dy(t)}{dt} + y(t) = K \cdot u(t). \tag{2}$$

Figure 4 shows the visualization of the PT1-approximation method. If a PT1-System is stimulated with a step function as the input function ( $u$ ), the step response as the output function ( $y$ ) is an exponential curve as illustrated in Fig. 4. The value ( $y_\infty = y(t \rightarrow \infty)$ ) is the saturation or final value of the step response and is assumed to be known or measurably known.

The parameters of the PT1 differential Eq. (2) may be derived using the equations  $K = \frac{\Delta y}{\Delta u}$  and  $T = T_{63\%} - T_0$ . The amplitude of the step function is referred to as  $\Delta u$ , and  $\Delta y$  denotes the difference between the final value  $y_\infty$  and the initial value  $y_0$ , prior to the step process beginning. The parameter  $T_0$  is the starting time of the step process, and in this case  $T_0 = 0$ . The parameter  $T_{63\%}$  indicates the time at which the step response reaches 63% of its final value.

The number 63% derives from the solution of the PT1 differential Eq. (2). Assuming that the input variable ( $u(t)$ ) is a unit step function, then the solution will be as follows:

$$y(t) = K \cdot \left(1 - e^{-\frac{t}{T}}\right).$$

Due to the unit step function, where  $\Delta u = 1$ ,  $K = \Delta y = y_\infty - y_0$ . In this case, it is assumed that  $y_0 = 0$ , consequently  $K = y_\infty$ . The previous equation may then be changed to:

$$y(t) = y_\infty \cdot \left(1 - e^{-\frac{t}{T}}\right).$$

For  $t = T$ :

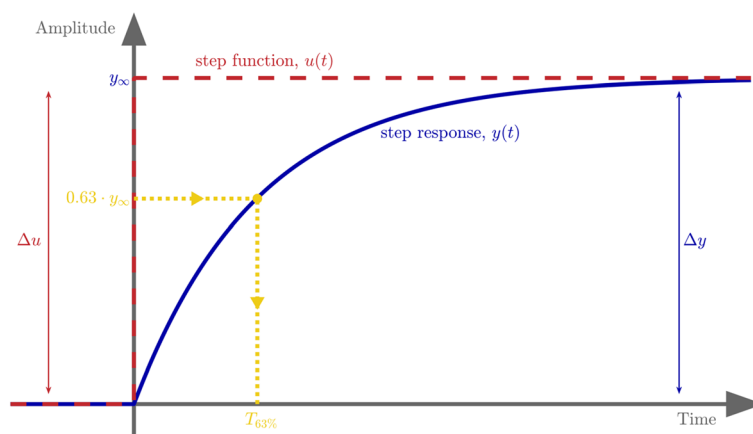


**Fig. 4** Visualization of the PT1-approximation method [53]

$$y(t = T) = y_{\infty} \cdot \left(1 - e^{-\frac{T}{T}}\right) = y_{\infty} \cdot \left(1 - e^{-1}\right) = 0.63 \cdot y_{\infty}.$$

Since it may be inferred to obtain the time constant of the PT1-system ( $T$ ),  $T_{63\%}$  must thus be computed.

This theory will now be applied to the actual measurements. The output variable ( $y$ ) reflects the preprocessed biogas production rate, while the input variable ( $u$ ) indicates the substrate feeding rate. The parameters  $K$  and  $T$  can be calculated from (Fig. 3). The difference in biogas production rate before and after the step process is referred to as  $\Delta y$  and subsequently  $\Delta u$  for substrate feeding rate. The step process begins on 29 September at around 08:00 (Fig. 3). Although it is a descending step as opposed to the upward step in Fig. 4, the modeling principle remains the same.

It is not suggested to compute  $\Delta y$  and  $\Delta u$  using only the first and last elements of the measurement data, as the outcome might not be optimal. This is one conclusion of the preliminary study, which is not displayed in this paper. Therefore,  $\Delta y$  and  $\Delta u$  will be determined by averaging the first and last  $p$ -elements from both measurement data (Algorithm 1, lines 3 and 4). The available data  $\mathfrak{P}$  must be considered while adjusting the hyperparameter  $p$ .

After calculating  $K$  and  $T$ , the differential Eq. (2) has been established. After that, it is possible to construct the continuous transfer function in the s-Laplace domain. This transfer function will be then converted into a discrete transfer function in the z-Laplace domain [55]. Finally, this discrete transfer function will be transformed back to the discrete-time domain, resulting in a difference Eq. (3).

$$\tilde{y}_k + a \cdot \tilde{y}_{k-1} = b \cdot u_{k-1} \tag{3}$$

$K$ ,  $T$  and the sampling time  $T_s$  may be used to derive the parameters  $a$  and  $b$ . Pseudo Code (Algorithm 1) illustrates the whole PT1-approximation estimation procedure.

---

**Algorithm 1:** System model estimation using PT1-approximation

---

**Input:**  $u_k, y_k, p, T_s$

- 1  $T_0$ : Start time of the step process
- 2  $T_{63\%}$ : Find the time when  $y_k$  has reached  $0.63 \cdot \lim_{k \rightarrow \infty} y_k$
- 3  $Biogas_{max} \cdot \frac{1}{p} \cdot \sum_{i=1}^p y_i, \quad Biogas_{min} \cdot \frac{1}{p} \cdot \sum_{i=\mathfrak{P}-p+1}^{\mathfrak{P}} y_i$
- 4  $Feeding_{max} \cdot \frac{1}{p} \cdot \sum_{i=1}^p u_i, \quad Feeding_{min} \cdot \frac{1}{p} \cdot \sum_{i=\mathfrak{P}-p+1}^{\mathfrak{P}} u_i$

// PT1-Approximation

- 5  $K = \frac{Biogas_{max} - Biogas_{min}}{Feeding_{max} - Feeding_{min}}, \quad T = T_{63\%} - T_0$
- 6 **Continuous transfer function:**  $G_c(s) = \frac{K}{T \cdot s + 1}$   
// Continuous-Discrete conversion
- 7 **Discrete transfer function:**  $G_d(z) = f(G_c(s), T_s) = \frac{b}{z + a}$   
// Discrete Laplace inverse transformation
- 8 **Difference equation:**  $\tilde{y}_k + a \cdot \tilde{y}_{k-1} = b \cdot u_{k-1}$

**Output:**  $G_d(z), \tilde{y}_k$

---

The algorithm's first two inputs are the biogas production rate ( $y_k$ ) and substrate mixture feeding rate ( $u_k$ ). Although both measurements are discrete, they will be handled as

continuous signals to determine the PT1 continuous transfer function. The outputs are the discrete transfer function ( $G_d(z)$ ) and the estimated biogas production rate ( $\tilde{y}_k$ ). The discrete transfer function is crucial for the feedback control design in the following subsection. The estimated biogas production rate ( $\tilde{y}_k$ ) can be compared with the measured biogas production rate ( $y_k$ ) to evaluate the estimation accuracy.

### Time percentage method

The measured biogas production rate will be approximated using the second-order differential Eq. (4) in the second approach based on the time percentage method.

$$(T_a \cdot T_b) \cdot \frac{d^2 y(t)}{dt^2} + (T_a + T_b) \cdot \frac{dy(t)}{dt} + y(t) = K \cdot u(t). \quad (4)$$

An advantage of this approach is more degrees of freedom compared to the PT1-approximation, and it is based on a second-order differential equation. However, having more degrees of freedom does not always imply that the time percentage method is more suited for modeling a biogas plant than the PT1-approximation. The modeling quality of all estimation methods will be provided in the “Results and discussion”.

Figure 5 shows the visualization of the time percentage method. The input function ( $u$ ) is a step function, same as the input function in Fig. 4. The step response ( $y$ ) will reach the setpoint or final value  $y_\infty$  outside of the displayed region. Because of clarity concerns, it is intended not to depict the whole step response.

The parameter  $K$  was computed in the same way as with PT1-approximation (Algorithm 1, lines 3–4). The time point that occurs when the biogas production rate reaches 72% of the intended setpoint is  $T_{72\%}$ , which is analogous to  $T_{63\%}$  from the previous technique. It is also possible to refer to the time at the first characteristic point ( $T_{72\%}$ ) as  $t_1$  and to deduce the time at the second characteristic point  $t_2 = 0.2847 \cdot t_1$  from it. The multiplication factor and the table (Table 2) were derived from the literature [52].

The next step is to read the biogas production rate ( $y_2$ ) by the time at the second characteristic point ( $t_2$ ). Since  $y_\infty$  is accessible from the chart (Fig. 3), it is possible to determine the ratio  $y_2/y_\infty$ . This ratio can be considered as an index for the lookup table (Table 2). The

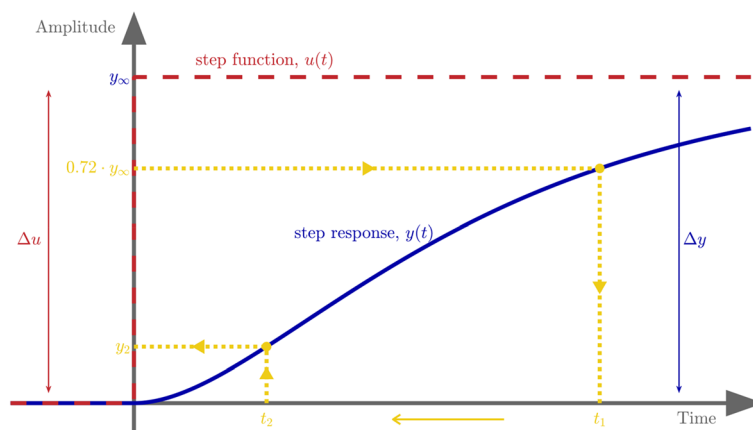


**Fig. 5** Visualization of the time percentage method [52]

**Table 2** Time constants for the time percentage method

$y_2/y_\infty$	$T_A/t_1$	$T_B/t_1$
0.3000	0.7950	0.000875
...	...	...
0.1610	0.3979	0.3979

row that corresponds to the calculated ratio will be selected and the values  $T_A/t_1$  and  $T_B/t_1$  can be extracted. Determining the time constants  $T_A$  and  $T_B$  comes as the last step.

The resulting continuous transfer function

$$G_c(s) = \frac{K}{(T_A \cdot s + 1) \cdot (T_B \cdot s + 1)}$$

is a PT2 element that consists of 2 PT1 elements connected in series. The whole procedure of the time percentage method is illustrated in the following Pseudo Code (Algorithm 2).

**Algorithm 2:** System model estimation using the time percentage method

```

Input:  $u_k, y_k, p, T_s$ , Tab. 2
1  $T_0$ : Start time of the step process
2  $T_{72\%} = t_1$ : Find the time when  $y_k$  has reached  $0.72 \cdot \lim_{k \rightarrow \infty} y_k$ 
3  $Biogas_{max} = \frac{1}{p} \cdot \sum_{i=1}^p y_i$ ,  $Biogas_{min} = \frac{1}{p} \cdot \sum_{i=p-p+1}^p y_i$ 
4  $Feeding_{max} = \frac{1}{p} \cdot \sum_{i=1}^p u_i$ ,  $Feeding_{min} = \frac{1}{p} \cdot \sum_{i=p-p+1}^p u_i$ 
// Time percentage method
5  $K = \frac{Biogas_{max} - Biogas_{min}}{Feeding_{max} - Feeding_{min}}$ 
6 Calculate  $t_2 = 0.2847 \cdot t_1$  and find  $y_2$  from  $y_k$ 
7 Calculate  $\frac{y_2}{y_\infty}$  and extract  $\frac{T_A}{t_1}, \frac{T_B}{t_1}$  from Tab. 2
8 Calculate  $T_A$  and  $T_B$  from the extracted parameters
9 Continuous transfer function:  $G_c(s) = \frac{K}{(T_A \cdot s + 1) \cdot (T_B \cdot s + 1)}$ 
// Continuous-Discrete conversion
10 Discrete transfer function:  $G_d(z) = f(G_c(s), T_s) = \frac{e \cdot z + f}{z^2 + c \cdot z + d}$ 
// Discrete Laplace inverse transformation
11 Difference equation:  $\tilde{y}_k + c \cdot \tilde{y}_{k-1} + d \cdot \tilde{y}_{k-2} = e \cdot u_{k-1} + f \cdot u_{k-2}$ 
Output:  $G_d(z), \tilde{y}_k$ 
    
```

**Summary of model estimation methods**

The following estimation techniques are the turning tangent method and the sum of time constants method. The turning point and turning tangent of the measured biogas production rate are crucial for the turning tangent method. The sum of time constants approach combines the time percentage method with the turning tangent method. The final techniques are PT1- and PT2-estimator, which differ significantly from the earlier estimating techniques. In this instance, the Least Squares (LS) approach will be applied to find the best fit to characterize the trajectory of the biogas production rate.

For this work, six estimation techniques have been implemented and compared. However, not all of them are covered in length in this paper for clarity. The optimum estimation model will then be determined by comparing the outcomes of these various estimation approaches. This will be explored in further detail in the section “[Results and discussion](#)”.

#### Methods 4: feedback control design

After a few examinations, two system models-one for the step upwards (second order differential equation) and one for the step downwards (first order differential equation)-are selected. The “[Results and discussion](#)” section will provide a detailed explanation, but the general idea is that two feedback controllers should be developed for each upward and downward model.

#### Feedback control system for downward model

This study suggests utilizing the Root Locus method and the Anti-Windup Scheme to develop discrete PI controllers [56] for the downward model. This subsection will present detailed steps to design this feedback control system.

The discrete transfer function

$$G_d(z) = \frac{b}{z + a}, \quad (5)$$

corresponds to a first-order differential equation model. This model Eq. (5) will be controlled by a PI-Controller Eq. (6) consisting of sampling time ( $T_s$ ), proportional ( $K_P$ ) and integral ( $K_I$ ) elements.

$$G_{PI}(z) = K_P + K_I \cdot T_s \cdot \frac{1}{z - 1}. \quad (6)$$

To reduce the degrees of freedom, the integral element  $K_I = \frac{1}{T_s}$  is chosen so that  $K_I \cdot T_s = 1$ . The PI-controller can be simplified to

$$G_{PI}(z) = K_P + \frac{1}{z - 1} = \frac{K_P \cdot z - K_P + 1}{z - 1} = K_P \cdot \frac{z + \frac{1 - K_P}{K_P}}{z - 1}. \quad (7)$$

The next step is calculating the proportional element  $K_P$ , for which one of the Root Locus construction rules is required [56].

#### Rules 1: Location of breakaway points

The breakaway points  $z$  (different from the zeros ( $\alpha$ ) and poles ( $\beta$ ) of the open loop system

$G_O(z) = G_{PI}(z) \cdot G_d(z)$ ) of the actual and complementary root locus follow from

$$\sum \frac{1}{z - \alpha} = \sum \frac{1}{z - \beta}$$

Implementing Rules 1 to Eqs. (5) and (7) leads to the following equation

$$\frac{1}{z+a} + \frac{1}{z-1} = \frac{1}{z + \frac{1-K_P}{K_P}} \quad (8)$$

The Eq. (8) can be simplified as follows:

$$z^2 - 2 \cdot \frac{1-K_P}{K_P} \cdot z - (1-a) \cdot \frac{1-K_P}{K_P} + a = 0. \quad (9)$$

Equation (9) illustrates that the change in  $K_P$  will cause the breakaway point to shift. Since it is a discrete model with a discrete controller, the optimal place for a breakaway point would be at the origin [57]. As a result, the  $K_P$  will be computed appropriately. Given that  $a$  is known, Eq. (9) can be transformed to solve for  $K_P$ :

$$-(1-a) \cdot \frac{1-K_P}{K_P} + a = 0 \Rightarrow K_P = 1-a.$$

Following establishing the breakaway point, moving the closed loop poles to the origin would be the next step. This necessitates the requirement for another Root Locus construction rule [56].

**Rules 2:** Parameterization of the root locus curve

The gain  $K_{RL}$  for a point  $z_1$  of the root locus is given by

$$K_{RL} = \frac{\prod |z_1 - \beta|}{\prod |z_1 - \alpha|}$$

The point  $z_1 = 0$  in this case, since the goal is to move all closed-loop poles to the origin. Implementing Rules 2 to Eqs. (5) and (7) results as follows:

$$K_{RL} \cdot b \cdot K_P = \frac{|0+a| \cdot |0-1|}{\left|0 + \frac{1-K_P}{K_P}\right|} \Rightarrow K_{RL} = \frac{-a}{(1-K_P) \cdot b}.$$

The PI-Controller has now been configured using the Root Locus method. Before designing the controller, it is vital to remember that the actual biogas plant has manipulated variable limitations. Some maximum and minimum values constrain the substrate mixture feeding rate. PI-Controller use in a system with a manipulated variable limit caused a Windup effect [58].

Consequently, an anti-Windup strategy must be established in the controller. Back Calculation (Fig. 6) is a traditional Anti-Windup approach proposed in this study that serves as a foundation for Anti-Windup in discrete controllers [59, 60]. The main concept is to avoid winding up the integrator component by subtracting the difference between the saturated and unsaturated manipulated variables. The Anti-Windup-Feedback is deactivated if there is no saturation. In the event of saturation, the Anti-Windup-Feedback limits

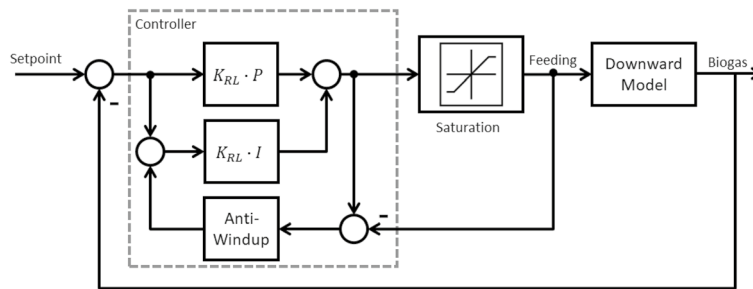


**Fig. 6** Feedback control loop using modified PI-Controller (downward model)

the integrator state. By setting the Anti-Windup-Gain to the inverse of the I-Controller  $K_{AW} = \frac{1}{K_I}$ , the whole feedback system will have the quickest step response possible [57].

**Feedback control system for upward model**

The primary principle for creating a feedback control system for an upward model is the same as for a downward model: design the controller so all closed loop poles are located in origin. Nevertheless, since the upward model is based on the second-order difference equation

$$G_d(z) = \frac{e \cdot z + f}{z^2 + c \cdot z + d}, \tag{10}$$

the upward model has a higher complexity than the downward model. This complexity pushes the root locus method to its limits. It is still possible to design a feedback control system using the root locus method, but moving all of the closed loop poles to the origin is impossible, even using a PID controller. Therefore, a state space controller will be designed for the upward model.

As this controller requires a system model in the state space form, Eq. (7) must first be transformed into a system of difference equations.

$$\begin{aligned} \mathbf{x}_{k+1} &= \underbrace{\begin{bmatrix} a_1 & a_2 \\ a_3 & a_4 \end{bmatrix}}_{\mathbf{A}} \cdot \mathbf{x}_k + \underbrace{\begin{bmatrix} b_1 \\ b_2 \end{bmatrix}}_{\mathbf{B}} \cdot \mathbf{u}_k \\ y_k &= \underbrace{[c_1 \ c_2]}_{\mathbf{C}} \cdot \mathbf{x}_k \end{aligned} \tag{11}$$

This Eq. (11) consists of a system matrix (**A**), input matrix (**B**), and output matrix (**C**). The controller is a gain matrix **K** such that the eigenvalues of  $\mathbf{A} - \mathbf{B} \cdot \mathbf{K} = \mathbf{0}$  [56]. These eigenvalues represent the closed-loop poles of the feedback control system and should lie at the origin, as mentioned earlier.

The structure of the state space controller is similar to that of the PD-controller, and the absence of an I-controller could result in a steady state error. Therefore, a pre-filter is required to drive this steady-state error to zero  $\mathbf{F} = [\mathbf{C} \cdot (\mathbf{B} \cdot \mathbf{K} - \mathbf{A})^{-1} \cdot \mathbf{B}]^{-1}$ . Figure 7 shows the design concept of this controller.

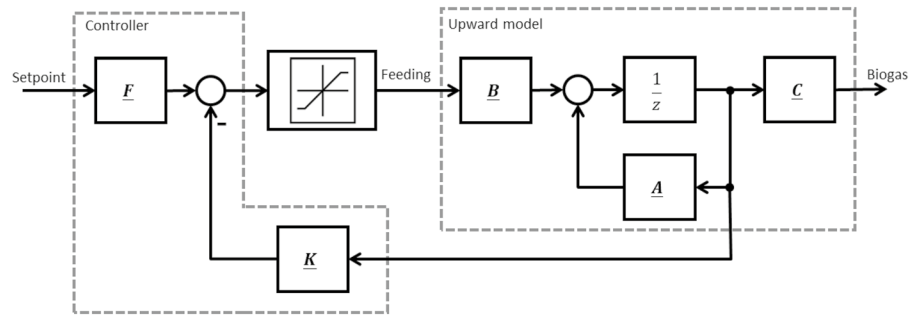


**Fig. 7** Feedback control loop using state space controller (upward model)

### Summary of feedback control design

Two controllers have been developed in this study: the modified PI controller for the downward model and the state space controller for the upward model. The subsequent algorithm (Algorithm 3) displays a Pseudo Code for both controllers.

---

#### Algorithm 3: Feedback controller

---

**Input:**  $G_d(z)$ ,  $T_s$ , **Fig. 6**, **Fig. 7**

// Downward model = PT1-approximation

1 **If** Downward model

2      $K_I = \frac{1}{T_s}$      // Integral element of the PI-controller

3      $K_P = 1 - a$      // Proportional element of the PI-controller

4      $K_{RL} = \frac{-a}{(1-K_P) \cdot b}$      // Root locus gain

5      $K_{AW} = \frac{1}{K_I}$      // Anti-Windup

6 **End**

// Upward model = Time percentage method

7 **If** Upward model

8     Transform the system model to (11)

9     Calculate a gain matrix  $\underline{K}$  such that the eigenvalues of  $\underline{A} - \underline{B} \cdot \underline{K} = \underline{0}$

10     Calculate the pre-filter:  $\underline{F} = [\underline{C} \cdot (\underline{B} \cdot \underline{K} - \underline{A})^{-1} \cdot \underline{B}]^{-1}$

11 **End**

// Simulation

12 Insert these parameters into the feedback control scheme **Fig. 6** or **Fig. 7**

13 Simulate and extract **substrate feeding plan** ( $\hat{u}_k$ )

**Output:**  $\hat{u}_k$

---

### Results and discussion

The methods have been established, and the outcomes are revealed in this section. First, the result of the model estimation will be shown and discussed. Subsequently, the feedback control design result will be presented from the simulation and the actual biogas plant.

**Results 1: model estimation**

The measurements from Fig. 3 will be inputs  $(u_k, y_k)$  to grade the quality of all model estimation methods. Only the best findings are displayed as figures (Fig. 8) in this paper for clarity reasons, and in this experiment, the PT1-approximation (Algorithm 1) delivers the best result.

The biogas production rate (blue line,  $y_k$ ), the substrate feeding rate (red line,  $u_k$ ), and the estimated biogas production rate (yellow line,  $\tilde{y}_k$ ) are the core information that can be extracted from the figure mentioned above. The grey dotted line depicts the biogas production rate at  $T_{63\%}$ , since it was the crucial parameter to be discovered when utilizing the PT1-approximation approach.

The abrupt change on 30 September represents a disturbance, as was stated in the previous section. The model, however, is robust enough and follows a similar trajectory to the actual measurement. This is due to the disturbance occurring after  $T_{63\%}$  and the substrate feeding rate returning to the prior level after the disturbance. The computed PT1-parameters  $K$  and  $T$  will therefore be the same as they would have been in the absence of any disturbance. The trajectory of the model estimation (yellow line) is calculated from the input (substrate feeding rate,  $u_k$ ) and the discrete transfer function  $G_d(z)$ . Despite not knowing that the blue line exists, this trajectory (yellow line) follows it closely.

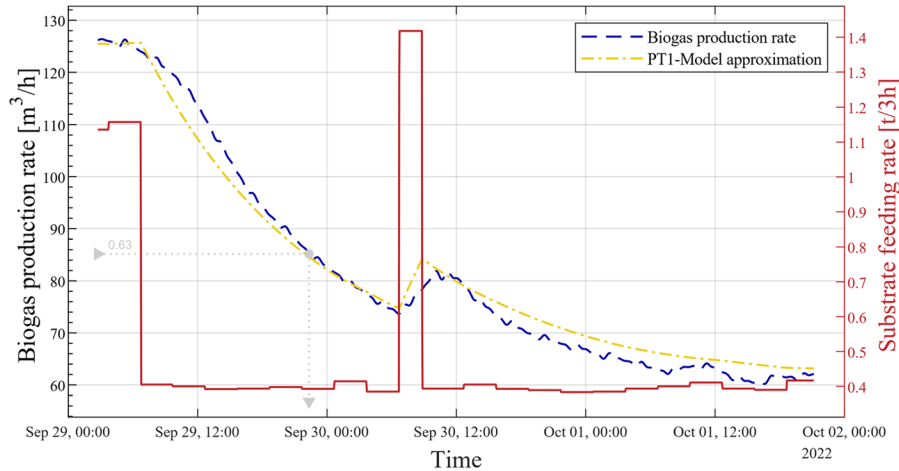


**Fig. 8** Downward model estimation using PT1-approximation

**Table 3** Evaluation criteria for downward model estimation

Estimation method	$R^2(\%)$	SSE(-)	P	AIC
PT1-approximation	99.04	38,071.82	2	29.38
Time percentage method	98.57	46,332.56	3	31.78
Turning tangent method	98.17	60,688.32	3	32.32
Sum of time constants method	98.17	60,668.62	3	32.32
PT1-estimator	96.03	263,158.74	2	33.25
PT2-estimator	97.78	391,200.21	4	38.04

In this paper, the Akaike Information Criterion (AIC) [61] is the primary evaluation criterion for selecting the best estimation method, a metric suitable for comparing regressions on nonlinear models. The sum of squares error (*SSE*)

$$SSE = \sum_k (y_k - \tilde{y}_k)^2,$$

and the number of model parameters (*P*) are required to calculate AIC. The following table (Table 3) displays the first experiment's results, and the coefficient of determination ( $R^2$ ) may also be obtained for comparison with AIC. The  $R^2$  value will not be considered an evaluation criterion since it is not a reliable indication of the fit quality for nonlinear models.

This result (Table 3) supports estimating a downward model using PT1-approximation since it has the lowest AIC value and, by coincidence, the highest  $R^2$  value.

The terms downward and upward models have appeared multiple times throughout the paper. The downward model is the estimation model from a step experiment to reduce the biogas production rate. Using the same analogy, the upward model is the estimation model from a step experiment to increase the biogas production rate. The distinction between these two scenarios is not required explicitly in a linear system. However, the linear models in this study are linearization of nonlinear systems. Therefore, at the very least, these two cases must be tested. The following figure (Fig. 9) displays the estimation result for the upward model.

This second experiment was conducted using a similar procedure as the first. The time percentage method (Algorithm 2) yielded the best result (Table 4), since it has the lowest AIC value. Table 4 shows that the PT2-estimator has the highest  $R^2$  value. However, its *SSE* value is significantly higher than the *SSE* value of the time percentage method. This situation strengthens the argument for using AIC as the primary criterion rather than  $R^2$  value.

The sum of time constants method requires the biogas production rate's turning point to determine the estimation model's order. Calculating the measurement's real turning point is problematic since the biogas production rate exhibits significant amplitude noise. The outcome was, therefore, inadequate.

The foundation of the time percentage method is the PT2-approximation, or second-order differential equation, with two different time constants  $T_A$  and  $T_B$ . One main distinction between a step response from a PT1 and PT2 system, is the tangent at the origin. It is zero for PT2-approximation and non-zero for PT1-approximation. This may explain why the time percentage method is more accurate than PT1-approximation for downward models.

If the substrate feeding were drastically reduced, the biogas production rate would almost immediately follow since the microorganisms would no longer have a food source and would hence produce less methane. If the substrate feeding were dramatically increased, the microorganisms would first need to digest the nutrition before increasing methane production. Or, to put it more simply, the PT1-approximation is the most effective for the downward model since the step reaction of a PT1 system operates instantly (non-zero tangent at the origin). The time percentage method works best for the upward model because the microorganisms need some time to produce more methane (zero tangent at the origin).

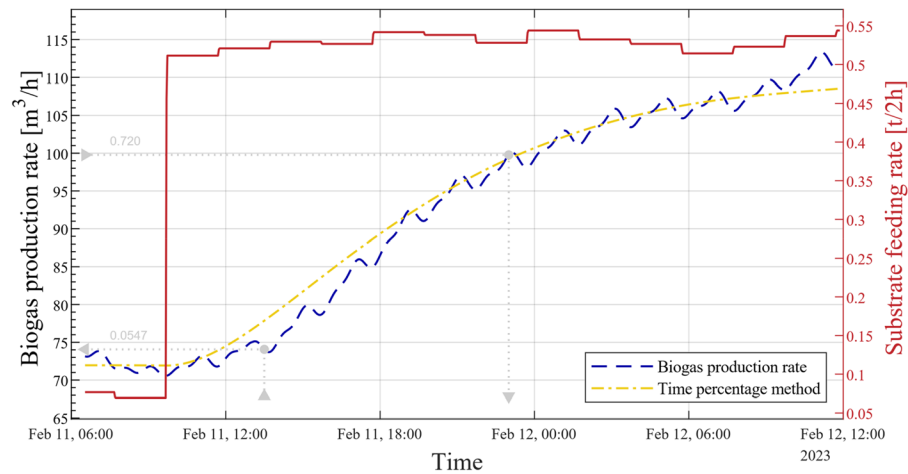


**Fig. 9** Upward model estimation using the time percentage method

**Table 4** Evaluation criteria for upward model estimation

Estimation method	$R^2(\%)$	$SSE(-)$	$P$	AIC
PT1-approximation	95.14	13,933.44	2	27.37
Time percentage method	98.73	3159.56	3	26.41
Turning tangent method	72.44	124,340.86	3	33.75
Sum of time constants method	6.91	–	3	–
PT1-estimator	97.65	144,225.25	2	32.05
PT2-estimator	98.94	671,858.91	4	39.13

Thus far, the models have been validated using their own training data, which was used to determine their model's parameters. Now, the estimation method will be validated using a new data set. During the experiment, the plant operator operated the biogas plant in such a scenario (Methods), allowing the step procedure to be readily carried out. Outside the experiment, the plant operator often changes the feeding rate based on the gas demand and the available substrate feeds. Furthermore, the plant operator feeds the plant at will, not adhering to the substrate mixtures (Table 1). The validation data was obtained outside of the experiment time since the experiment time was limited.

The requirements for validation data are:

- The plant was fed with one of the substrate mixtures (Table 1).
- The substrate feeding rate exhibits step-function behavior.

These considerations led to selecting specific days, from 18 to 20 February, to validate the upward model estimation. However, no validation data was available for the downward model estimation. As noted earlier, the upward model estimation was selected using the time percentage method, and the validation result is shown in Fig. 10.

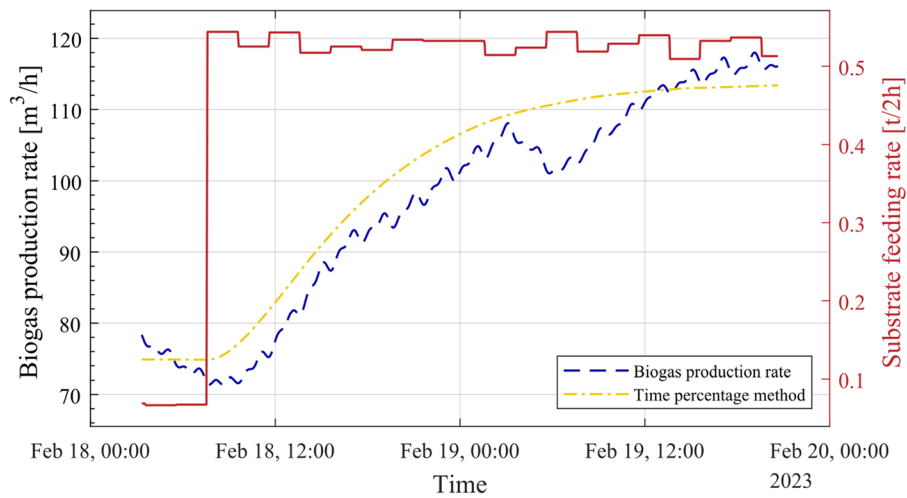


**Fig. 10** Upward model estimation against a new data set

As observed, the substrate feeding rate exhibits a step-like behavior in this situation. The fluctuation following the step event was modest; therefore, the feeding rate may be presumed to remain constant both before and after the step event. Fortunately, as the selected data occurs one week after the second experiment (Fig. 9), the plant operator continues employing identical substrate mixtures as in the second experiment. Since the two requirements were fulfilled, 18 February through 20 February was selected as the validation data.

The new substrate feeding rate (red line,  $u_k$ ) is now used as the input to the system model, using the time percentage method. It should be noted that the model's parameters are not modified. They remain unchanged as in Fig. 9. The model's output is the estimated biogas production rate (yellow line,  $\tilde{y}_k$ ) and the trajectory resembles the actual biogas production rate (blue line,  $y_k$ ). Table 5 displays the evaluation values against the new 18–20 February data set.

The coefficient of determination ( $R^2$ ) and the mean absolute error (MAE)

$$MAE = \frac{\sum_{k=1}^{\mathfrak{P}} |y_k - \tilde{y}_k|}{\mathfrak{P}},$$

are used to quantify the model's fitting quality, with  $\mathfrak{P}$  = the total number of measurements. The  $R^2$  value of 94.9% indicates the similarity of the estimated and the actual biogas production rates, and the mean absolute error between them is  $4.01 \frac{\text{m}^3}{\text{h}}$ . This indicates that the model can forecast the actual biogas production rate with an average inaccuracy of  $4.01 \frac{\text{m}^3}{\text{h}}$ . The AIC values are not displayed in Table 5 since they are used to compare models, and in this instance, the model has already been selected.

**Table 5** Evaluation values for upward model estimation against a new data set

Estimation method	$R^2$ (%)	MAE ( $\text{m}^3/\text{h}$ )
Time percentage method	94.9	4.01

### Results 2: feedback control design

The system models have been established, and the feedback control design will now be evaluated. As previously noted, the downward model (PT1-approximation) is controlled by the PI controller using the Root Locus method and Anti-Windup Scheme (Fig. 6). The following figure (Fig. 11) displays the simulation result.

The setpoint is represented as the red line that symbolizes a step down from  $126 \frac{\text{m}^3}{\text{h}}$  to  $66 \frac{\text{m}^3}{\text{h}}$ . The blue line represents the simulated biogas production using a modified PI-controller and as a comparison, the simulated biogas production using a deadbeat controller is shown with the yellow line. The deadbeat controller is one of the most well-known controllers in discrete control theory and is used in this paper for comparing the selected controller with a standard one.

The oscillation / Windup behavior is the main drawback of employing a deadbeat controller with manipulated variable limitations. This behavior indicates that the controller's calculated substrate feeding schedule also oscillates. Avoiding this negative behavior at all costs is advisable.

The PI controller exhibits quick step responses, non-oscillating behavior, and simple implementation. Consequently, it is selected as the feedback controller for the downward model.

The state space controller controls the upward model (Fig. 7), and the following figure (Fig. 12) displays the simulation result. The setpoint is a step upward from  $64 \frac{\text{m}^3}{\text{h}}$  to  $94 \frac{\text{m}^3}{\text{h}}$  and is represented as a red line. The green line shows the simulated biogas production rate using the selected state space controller. For comparison, the yellow line portrays the result from the deadbeat controller, and the blue line is from the modified PI controller.

This graph makes it apparent why the state space controller was selected as the controller for the upward model in this study. In addition to having the quickest step response, it behaves in a non-oscillating and non-all-pass manner.

Having achieved such positive simulation results, the project is progressing with testing the controller on the actual biogas plant. Due to the substrate feeding options available then, the experiment could only be conducted using substrate mixture 1 (Table 1). The substrate mixture 1 was supplied to the plant three days before the experiment. During this preparation stage, the plant operator can flexibly alter the amount of substrate feeding as long as the relative mixtures remain constant. After three days, the experiment used a downward model to decrease the biogas production rate. The initial biogas production rate was extracted from the PLC ( $\approx 126 \frac{\text{m}^3}{\text{h}}$ ) and the setpoint will be  $88 \frac{\text{m}^3}{\text{h}}$ . This value was primarily decided based on how long it would take for the biogas production rate to reach the desired setpoint. The background is purely practical, as the plant operator must supervise the entire experiment, and hence, the experiment can only be performed during working hours.

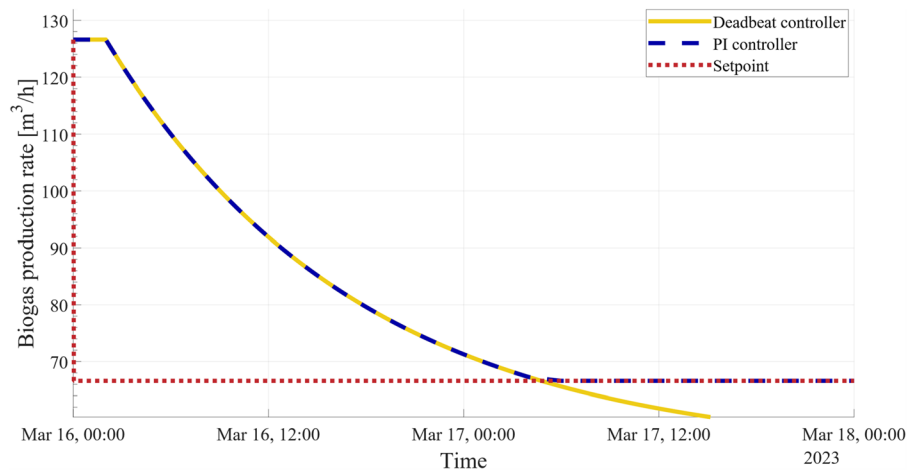


**Fig. 11** Modified PI-controller for downward model

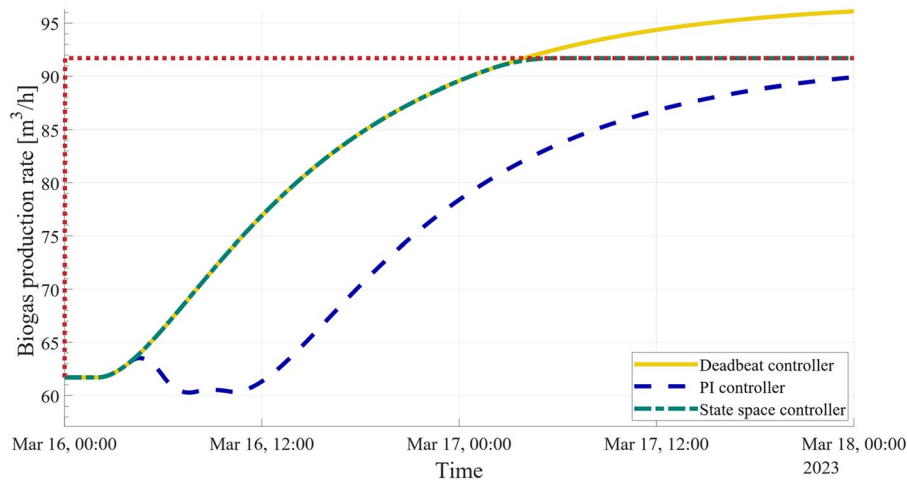


**Fig. 12** State-space controller for upward model

The simulation was run using this setpoint and initial states of the plant, and the outcome of the controller is a two-hourly feeding schedule (Table 6). Four schedule segments are displayed on the right side of the table. The schedule changes only between the segments, not within one segment. The first segment describes the initial state of the substrate feeding rate, and the rest of the segment explains the controller plan to reduce the biogas production rate to  $88 \frac{m^3}{h}$ .

A schedule should be created as precisely as feasible so the plant operator can operate it efficiently. Early in the morning, the plant operator would place 2318.7 kg corn, 1391.2 kg manure, and 463.7 kg Grass silage and fodder residues (Table 6, last row) into a mixing tank. The plant operator would then program the automatic feeder to start feeding the plant with 758 kg of this mixture at 08:00, 100 kg for the following 8 h, 234 kg at 18:00, and 463.6 kg for the remainder of the day until 6:00 the next day. Every plant

**Table 6** Two-hourly feeding schedule, the controller output

Time	Corn (kg)	Manure (kg)	Grass silage & fodder residues (kg)	Sum (kg)
08:00	421.1	252.7	84.2	758
10:00	55.6	33.3	11.1	100
12:00	55.6	33.3	11.1	100
14:00	55.6	33.3	11.1	100
16:00	55.6	33.3	11.1	100
18:00	130	78	26	234
20:00	257.6	154.5	51.5	463.6
22:00	257.6	154.5	51.5	463.6
...	...	...	...	...
06:00 + 1d	257.6	154.5	51.5	463.6
Sum (daily)	2318.7	1391.2	463.7	4173.7

operator can follow this schedule; the sole component required is an automatic feeder, already present in the biogas plant Grub.

Figure 13 shows the outcome of using the schedule mentioned earlier in the biogas plant Grub. The segments of the feeding schedule are displayed beneath the abscissa. Since Fig. 13 starts earlier, at midnight (00:00), the first segment is longer than in Table 6 (beginning at 08:00). During the first segment, the substrate feeding rate remains constant from midnight until 08:00. However, it is apparent that there are minor changes within one segment (red line). It is primarily due to uncertainty in the mixing tank’s scale and the automatic feeder.

The setpoint (blue line) is an artificial line that displays the biogas production rate’s starting point and target value. The biogas production rate (yellow line) gradually decreases as it gets closer to the target value. However, since the amplitude of the biogas production rate can be influenced by the lowpass and smoothing filter, it could be a coincidence that the biogas production rate precisely matches the target value at the end of the experiment. Furthermore, since it appears that it has yet to reach the saturation stage, a more extended experiment might see a further decline in the biogas production rate.

The experiment was terminated on 17 March, at 06:00, since it was a Friday and the plant operator needed to prepare for the weekend. This experiment raises questions that must be addressed soon, such as why the biogas production rate started declining in segment 1 even though the substrate feeding rate remained constant. Additionally, the biogas production rate is still falling in segment 4, and an increase in the substrate feeding rate from segments 2–4 appears to have little effect on this trajectory.

An improvement would be possible if the initial measurement values for the biogas production and substrate feeding rates could be derived in real-time. The biogas plant’s data is only updated twice daily, and the initial values may not match the actual measurements. Another potential improvement is updating the system model (Fig. 8), which was developed six months before this experiment.

The estimation of the model should also take the state of the biogas plant into account. The acetic acid concentration, temperature, pH level, VFA/TA ratio, and dry

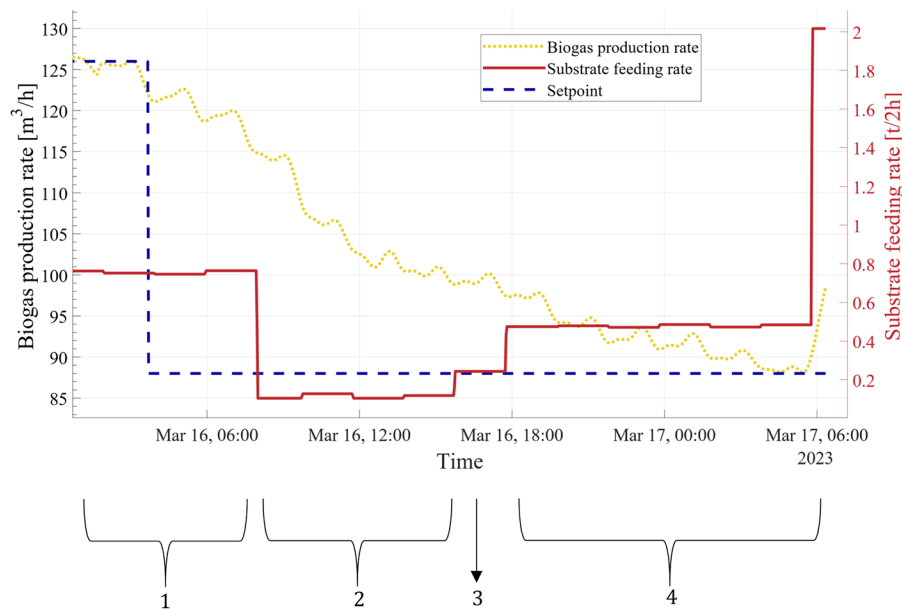


**Fig. 13** Experiment results in the biogas plant Grub using a modified PI-controller

matter all have a role in the biogas plant's state. These values might be measured in the laboratory or estimated using a NIR sensor and machine learning [62–65]. The state of the biogas plant should be considered while using the system model estimation method as the plant's operating points of linearization.

Finally, further study is required to discover a single control system that can handle both upward and downward models. The state space controller could also control the downward model; however, the absence of an I-controller could result in a steady state error. Future research will determine whether a PI-controller, state space controller, and Anti-Windup scheme combination can solve the issue.

Nevertheless, this experiment demonstrated the possibility of controlling a biogas plant using a modest feedback control system, and demand-oriented flexibilization could be accomplished soon.

## Conclusion

The project aims to create an intuitive yet precise feedback control system for demand-oriented biogas production utilizing actual data from the biogas plant Grub. Before proceeding to the subsequent phases, the raw data must first be preprocessed. The biogas production rate was filtered using lowpass and smoothing filters to reduce heavy noise associated with the measurement data. The PLC measures and records the biogas production, and a discrete derivative was performed to calculate the biogas production rate. The derivation was subsequently examined for coherence and consistency using further batch processing.

This study employs the Grey-Box method to take the structure of the anaerobic digestion model from the White-Box method, neglecting the assumed constant parameters so that the system model only has one input (substrate mixture feeding rate) and one output (biogas production rate), and then uses statistical data from the Black-Box method

to identify a correlation between the model's input and output. This paper differs from other literature, considering a mixture of different substrates as one input rather than one per substrate. A total of six estimation methods were calculated to determine which system model best described the mathematical connection between the substrate feeding rate and biogas production rate.

These estimation methods were based on step inputs and step responses from control theory. Steps downward were best approximated with PT1-approximation and upward with the time percentage method, based on the second-order differential equation. The Akaike Information Criterion is the main factor for determining the optimal approximation method.

A state-space controller controls the upward model, whereas the downward model is controlled by a discrete PI controller using the Root Locus method and Anti-Windup Scheme. The simulation outcomes demonstrated that both controllers could determine the quickest step response and exhibit non-oscillatory behavior. The algorithm was tested in an actual biogas plant in Grub, and the initial evaluation indicated that it could decrease the biogas production rate to a level close to the setpoint within the estimated time.

#### Abbreviations

ADM1	Anaerobic digestion model no. 1
AI	Artificial intelligence
AIC	Akaike information criterion
BMP	Biochemical methane potential
CHP	Combined heat and power
EEG	Renewable energy sources act
MAE	Mean absolute error
MPC	Model predictive control
PI	Proportional-integral controller
PID	Proportional-integral-derivative controller
PLC	Programmable logic controller
SSE	Sum of squares error
TA	Total alkalinity
VFA	Volatile fatty acid

#### Symbols

$a, \dots, f$	Difference equation parameters
$\underline{A}$	System matrix
$\underline{B}$	Input matrix
$\underline{C}$	Output matrix
$\underline{F}$	Pre-filter of the state space controller
$\bar{G}_c(s)$	Continuous transfer function
$G_d(z)$	Discrete transfer function
$G_{PI}(z)$	Discrete transfer function of the PI controller
$K$	Gain parameter of the estimation model
$\underline{K}$	Gain matrix of the state space controller
$K_{AW}$	Anti-windup gain
$K_I$	Integral element of the PI controller
$K_P$	Proportional element of the PI controller
$K_{RL}$	Root locus gain
$n$	The order of the differential equation
$p$	Number of measurements to be considered for calculations lines 3, 4 in Algorithm 1 and Algorithm 2
$P$	Number of model parameters
$\mathfrak{P}$	Total number of measurements
$R^2$	Coefficient of determination
$s$	Continuous Laplace variable
$t_1, t_2$	Characteristic points for the time percentage method
$T$	Time constant of PT1-approximation
$T_a, T_b$	Time constants of the time percentage method
$T_s$	Sampling time
$T_0$	Time when the step-process begins
$T_{63\%}$	Time when the biogas production rate has reached 63% of the desired setpoint value
$T_{72\%}$	Time when the biogas production rate has reached 72% of the desired setpoint value

$u_k$	Substrate mixture feeding rate
$\hat{u}_k$	Substrate mixture feeding rate, the controller output
$\mathbf{x}_k$	State vector
$y_k$	Biogas production rate
$\tilde{y}_k$	Estimated biogas production rate
$z$	Discrete Laplace variable

**Greek letters**

$\alpha$	Zeros of the open loop system $G_O(z)$
$\beta$	Poles of the open loop system $G_O(z)$
$\Delta$	Values difference between before and after the step-process

**Sub- and Superscripts**

$k$	Discrete variable
-----	-------------------

**Acknowledgements**

Many thanks to the industrial partners from this project: ib-comPLAN and Bayerische Staatsgüter, who helped to collect the data from the biogas plant and to perform the experiments.

**Author contributions**

LAP analyzed and interpreted the data from the biogas plant. He then developed all the estimation models and the feedback control system. He was a major contributor in writing the manuscript. BH wrote the project proposal and made this project possible. He then prepared and organized the experiments at the biogas plant and contributed to editing the manuscript. MG contributed to the idea of the proposal and contributed to editing the manuscript. All authors read and approved the final manuscript.

**Funding**

Open Access funding enabled and organized by Projekt DEAL. Supported by the Federal Ministry of Food and Agriculture and Fachagentur Nachwachsende Rohstoffe. Funding reference: 2220NR046A.

**Availability of data and materials**

The data that support the finding of this study are available from the biogas plant Grub, but restrictions apply to the availability of these data, which were used under license for the current study, and so are not publicly available. Data are, however, available from the authors upon reasonable request and with permission of the biogas plant Grub.

**Declarations****Competing interests**

The authors declare that they have no competing interests.

Received: 18 July 2023 Accepted: 18 September 2023

Published online: 27 November 2023

**References**

- Stitt J. Germany's Erneuerbare-Energien-Gesetz and Incentives for Renewable Energy Production. 2022.
- Presse- und Informationsamt der Bundesregierung. We're tripling the speed of the expansion of renewable energies. 2022.
- Görsch U, Helm M, editors. Biogasanlagen: Planung, Errichtung und Betrieb von landwirtschaftlichen und industriellen Biogasanlagen; 13 Tabellen. 3rd ed. Stuttgart: Ulmer; 2014.
- Tabatabaei M, Ghanavati H. Biogas. Cham: Springer International Publishing; 2018.
- Deublein D, editor. Biogas from waste and renewable resources: an introduction. 1st ed. Weinheim: Wiley; 2008.
- Batstone DJ, Keller J, Angelidaki I, Kalyuzhnyi SV, Pavlostathis SG, Rozzi A, et al. The IWA anaerobic digestion model no 1 (ADM1). *Water Sci Technol.* 2002;45:65–73. <https://doi.org/10.2166/wst.2002.0292>.
- Ramirez I, Mottet A, Carrère H, Déléris S, Vedrenne F, Steyer J-P. Modified ADM1 disintegration/hydrolysis structures for modeling batch thermophilic anaerobic digestion of thermally pretreated waste activated sludge. *Water Res.* 2009;43:3479–92. <https://doi.org/10.1016/j.watres.2009.05.023>.
- Li X, Yang Z, Liu G, Ma Z, Wang W. Modified anaerobic digestion model No. 1 (ADM1) for modeling anaerobic digestion process at different ammonium concentrations. *Water Environ Res.* 2019;91:700–14. <https://doi.org/10.1002/wer.1094>.
- Donoso-Bravo A, Sadino-Riquelme MC, Valdebenito-Rolack E, Paulet D, Gómez D, Hansen F. Comprehensive ADM1 extensions to tackle some operational and metabolic aspects in anaerobic digestion. *Microorganisms.* 2022. <https://doi.org/10.3390/microorganisms10050948>.
- Yasui H, Goel R, Li YY, Noike T. Modified ADM1 structure for modelling municipal primary sludge hydrolysis. *Water Res.* 2008;42:249–59. <https://doi.org/10.1016/j.watres.2007.07.004>.
- Weinrich S, Mauky E, Schmidt T, Krebs C, Liebetrau J, Nelles M. Systematic simplification of the Anaerobic Digestion Model No. 1 (ADM1)—Laboratory experiments and model application. *Bioresour Technol.* 2021;333:125104. <https://doi.org/10.1016/j.biortech.2021.125104>.

12. Hassam S, Ficara E, Leva A, Harmand J. A generic and systematic procedure to derive a simplified model from the anaerobic digestion model No. 1 (ADM1). *Biochem Eng J.* 2015;99:193–203. <https://doi.org/10.1016/j.bej.2015.03.007>.
13. Li D, Lee I, Kim H. Application of the linearized ADM1 (LADM) to lab-scale anaerobic digestion system. *J Environ Chem Eng.* 2021;9: 105193. <https://doi.org/10.1016/j.jece.2021.105193>.
14. Budhijanto W, Purnomo CW, Siregar NC. Simplified mathematical model for quantitative analysis of biogas production rate in a continuous digester. *EJ.* 2012;16:167–76. <https://doi.org/10.4186/ej.2012.16.5.167>.
15. Razaviarani V, Buchanan ID. Calibration of the Anaerobic Digestion Model No. 1 (ADM1) for steady-state anaerobic co-digestion of municipal wastewater sludge with restaurant grease trap waste. *Chem Eng J.* 2015;266:91–9. <https://doi.org/10.1016/j.cej.2014.12.080>.
16. Bornhöft A, Hanke-Rauschenbach R, Sundmacher K. Steady-state analysis of the Anaerobic Digestion Model No. 1 (ADM1). *Nonlinear Dyn.* 2013;73:535–49. <https://doi.org/10.1007/s11071-013-0807-x>.
17. Souza TSO, Carvajal A, Donoso-Bravo A, Peña M, Fdz-Polanco F. ADM1 calibration using BMP tests for modeling the effect of autohydrolysis pretreatment on the performance of continuous sludge digesters. *Water Res.* 2013;47:3244–54. <https://doi.org/10.1016/j.watres.2013.03.041>.
18. Poggio D, Walker M, Nimmo W, Ma L, Pourkashanian M. Modelling the anaerobic digestion of solid organic waste—substrate characterisation method for ADM1 using a combined biochemical and kinetic parameter estimation approach. *Waste Manag.* 2016;53:40–54. <https://doi.org/10.1016/j.wasman.2016.04.024>.
19. Arnell M, Astals S, Åmand L, Batstone DJ, Jensen PD, Jeppsson U. Modelling anaerobic co-digestion in Benchmark Simulation Model No. 2: parameter estimation, substrate characterisation and plant-wide integration. *Water Res.* 2016;98:138–46. <https://doi.org/10.1016/j.watres.2016.03.070>.
20. Lübken M, Koch K, Gehring T, Horn H, Wichern M. Parameter estimation and long-term process simulation of a biogas reactor operated under trace elements limitation. *Appl Energy.* 2015;142:352–60. <https://doi.org/10.1016/j.apenergy.2015.01.014>.
21. Batstone DJ, Torrijos M, Ruiz C, Schmidt JE. Use of an anaerobic sequencing batch reactor for parameter estimation in modelling of anaerobic digestion. *Water Sci Technol.* 2004;50:295–303. <https://doi.org/10.2166/wst.2004.0663>.
22. Bai J, Liu H, Yin B, Ma H. Modeling of enhanced VFAs production from waste activated sludge by modified ADM1 with improved particle swarm optimization for parameters estimation. *Biochem Eng J.* 2015;103:22–31. <https://doi.org/10.1016/j.bej.2015.06.015>.
23. Bechara R. Improvements to the ADM1 based Process Simulation Model: reaction segregation, parameter estimation and process optimization. *Heliyon.* 2022;8: e11793. <https://doi.org/10.1016/j.heliyon.2022.e11793>.
24. Ahmed W, Rodríguez J. Generalized parameter estimation and calibration for biokinetic models using correlation and single variable optimisations: application to sulfate reduction modelling in anaerobic digestion. *Water Res.* 2017;122:407–18. <https://doi.org/10.1016/j.watres.2017.05.067>.
25. Raeyatdoost N, Bongards M, Bäck T, Wolf C. Robust state estimation of the anaerobic digestion process for municipal organic waste using an unscented Kalman filter. *J Process Control.* 2023;121:50–9. <https://doi.org/10.1016/j.jprocont.2022.11.013>.
26. Yang C, Seiler P, Belia E, Daigger GT. An adaptive real-time grey-box model for advanced control and operations in WRRFs. *Water Sci Technol.* 2021;84:2353–65. <https://doi.org/10.2166/wst.2021.408>.
27. Montiel-Escobar JL, Alcaraz-González V, Méndez-Acosta HO, González-Álvarez V. ADM1-based robust interval observer for anaerobic digestion processes. *Clean: Soil, Air, Water.* 2012;40:933–40. <https://doi.org/10.1002/clen.201100718>.
28. Sbarciog M, Giovannini G, Chamy R, Wouwer AV. Control and estimation of anaerobic digestion processes using hydrogen and volatile fatty acids measurements. *Water Sci Technol.* 2018;78:2027–35. <https://doi.org/10.2166/wst.2018.465>.
29. Kamarád L, Pohn S, Bochmann G, Harasek M. Determination of mixing quality in biogas plant digesters using tracer tests and computational fluid dynamics. *Acta Univ Agric Silv Mendelianae Brun.* 2013;61:1269–78. <https://doi.org/10.11118/actaun201361051269>.
30. Li L, Wang K, Zhao Q, Gao Q, Zhou H, Jiang J, Mei W. A critical review of experimental and CFD techniques to characterize the mixing performance of anaerobic digesters for biogas production. *Rev Environ Sci Biotechnol.* 2022;21:665–89. <https://doi.org/10.1007/s11157-022-09626-z>.
31. Singh B, Szamosi Z, Siménfalvi Z. Impact of mixing intensity and duration on biogas production in an anaerobic digester: a review. *Crit Rev Biotechnol.* 2020;40:508–21. <https://doi.org/10.1080/07388551.2020.1731413>.
32. Brito-Espino S, García-Ramírez T, Leon-Zerpa F, Mendieta-Pino C, Santana JJ, Ramos-Martín A. E-Learning proposal for 3D modeling and numerical simulation with FreeFem++ for the study of the discontinuous dynamics of biological and anaerobic digesters. *Water.* 2023;15:1181. <https://doi.org/10.3390/w15061181>.
33. Arnau R, Climent J, Martínez-Cuenca R, Rodríguez J, Chiva S. Evaluation of hydraulic mixing performance in a full-scale anaerobic digester with an external liquid recirculation system using CFD and experimental validation. *Chem Eng Sci.* 2022;251: 117392. <https://doi.org/10.1016/j.ces.2021.117392>.
34. Beltramo T, Klocke M, Hitzmann B. Prediction of the biogas production using GA and ACO input features selection method for ANN model. *Inform Process Agric.* 2019;6:349–56. <https://doi.org/10.1016/j.inpa.2019.01.002>.
35. Cinar S, Cinar SO, Wieczorek N, Sohoo I, Kuchta K. Integration of artificial intelligence into biogas plant operation. *Processes.* 2021;9:85. <https://doi.org/10.3390/pr9010085>.
36. Long F, Wang L, Cai W, Lesnik K, Liu H. Predicting the performance of anaerobic digestion using machine learning algorithms and genomic data. *Water Res.* 2021;199: 117182. <https://doi.org/10.1016/j.watres.2021.117182>.
37. Xu W, Long F, Zhao H, Zhang Y, Liang D, Wang L, et al. Performance prediction of ZVI-based anaerobic digestion reactor using machine learning algorithms. *Waste Manag.* 2021;121:59–66. <https://doi.org/10.1016/j.wasman.2020.12.003>.
38. Rieke C, Stollenwerk D, Dahmen M, Pieper M. Modeling and optimization of a biogas plant for a demand-driven energy supply. *Energy.* 2018;145:657–64. <https://doi.org/10.1016/j.energy.2017.12.073>.

39. Zuru AA, Dangoggo SM, Birnin-Yauri UA, Tambuwal AD. Adoption of thermogravimetric kinetic models for kinetic analysis of biogas production. *Renewable Energy*. 2004;29:97–107. [https://doi.org/10.1016/S0960-1481\(03\)00074-0](https://doi.org/10.1016/S0960-1481(03)00074-0).
40. Schelo T, Bidel A, Hamacher T. Biogas plant operation under distribution locational marginal prices. In: 2021 IEEE Madrid PowerTech; 28.06.2021–02.07.2021; Madrid, Spain: IEEE; 6282021. p. 1–6. <https://doi.org/10.1109/PowerTech46648.2021.9494774>.
41. Peters L, Biernacki P, Uhlenhut F, Steinigeweg S. Modelling of demand driven biogas plants to cover residual load rises. In: The economy, sustainable development, and energy international conference. Basel Switzerland: MDPI; 2018. p. 1385. <https://doi.org/10.3390/proceedings2221385>.
42. Expected hypervolume improvement algorithm for PID controller tuning and the multiobjective dynamical control of a biogas plant: IEEE; 2015.
43. Mauky E, Weinrich S, Nägele H-J, Jacobi HF, Liebetrau J, Nelles M. Model predictive control for demand-driven biogas production in full scale. *Chem Eng Technol*. 2016;39:652–64. <https://doi.org/10.1002/ceat.201500412>.
44. Mauky E. null model-based control concept for a demand-driven biogas production: Universität Rostock; 2018.
45. Nonlinear model predictive substrate feed control of biogas plants: IEEE; 2012.
46. Haugen F, Bakke R, Lie B. State estimation and model-based control of a pilot anaerobic digestion reactor. *J Contr Sci Eng*. 2014;2014:1–19. <https://doi.org/10.1155/2014/572621>.
47. Scherer P, Schreiber A, Arthur R, Antonczyk S, Vollmer G-R. Doubling the space-time yield of a pilot biogas reactor with swine manure and cereal residues by a closed loop feedback control based on an automated fuzzy logic control system. *Processes*. 2022;10:2511. <https://doi.org/10.3390/pr10122511>.
48. Biogas Intelligence-operate biogas plants using Neural Network and Fuzzy logic: IEEE; 2013.
49. Lichti F, Tappen S, Schober J. Einrichtung und Erprobung des Intervallbetriebs der Biogasanlage an der Versuchsstation Grub. Abschlussbericht zum Vorhaben. 2018.
50. Meyer M. Signalverarbeitung. Wiesbaden: Vieweg+Teubner; 2011.
51. Frey T, Bossert M. Signal- und Systemtheorie. Wiesbaden: Vieweg+Teubner; 2009.
52. Praktische Regelungstechnik. Wiesbaden: Vieweg+Teubner; 2008.
53. Lunze J. Regelungstechnik. Berlin: Springer; 2014.
54. Isermann R, Münchhof M. Identification of dynamic systems. Berlin: Springer; 2011.
55. Föllinger O, Kluwe M. Laplace-, Fourier- und z-Transformationen. 8th ed. Heidelberg: Hüthig; 2003.
56. Adamy J. Systemdynamik und Regelungstechnik II. 6th ed. Düren: Shaker; 2019.
57. Konigorski U. Digitale Regelungssysteme I und II: Skript zur Vorlesung, Sommersemester 2020: Technische Universität, Institut für Automatisierungstechnik, FG; 2020.
58. Adamy J. Nichtlineare systeme und regelungen. Berlin: Springer; 2014.
59. Fertik HA, Ross CW. Direct digital control algorithm with anti-windup feature. *ISA Trans*. 1967;6:317–20.
60. Ortseifen A. Entwurf von modellbasierten Anti-Windup-Methoden für Systeme mit Stellbegrenzungen: VDI Verlag GmbH; 2013.
61. Spiess A-N, Neumeyer N. An evaluation of R2 as an inadequate measure for nonlinear models in pharmacological and biochemical research: a Monte Carlo approach. *BMC Pharmacol*. 2010;10:6. <https://doi.org/10.1186/1471-2210-10-6>.
62. Putra LA, Huber B, Gaderer M. Estimation of acetic acid concentration from biogas samples using machine learning. *Int J Chem Eng*. 2023;2023:1–11. <https://doi.org/10.1155/2023/2871769>.
63. Stockl A, Oechsner H. Near-infrared spectroscopic online monitoring of process stability in biogas plants. *Eng Life Sci*. 2012;12:295–305. <https://doi.org/10.1002/elsc.201100065>.
64. Krapf LC, Gronauer A, Schmidhalter U, Heuwinkel H. Near infrared spectroscopy calibrations for the estimation of process parameters of anaerobic digestion of energy crops and livestock residues. *J Near Infrared Spectrosc*. 2011;19:479–93. <https://doi.org/10.1255/jnirs.960>.
65. Krapf LC, Gronauer A, Schmidhalter U, Heuwinkel H. Evaluation of agricultural feedstock-robust near infrared calibrations for the estimation of process parameters in anaerobic digestion. *J Near Infrared Spectrosc*. 2012;20:465–76. <https://doi.org/10.1255/jnirs.1013>.

## Publisher's Note

Springer Nature remains neutral with regard to jurisdictional claims in published maps and institutional affiliations.

Submit your manuscript to a SpringerOpen<sup>®</sup> journal and benefit from:

- Convenient online submission
- Rigorous peer review
- Open access: articles freely available online
- High visibility within the field
- Retaining the copyright to your article

---

Submit your next manuscript at ► [springeropen.com](https://www.springeropen.com)

---